Anal. Chem. **1997,** *69,* 3959−3965

Combined Ion Mobility/Time-of-Flight Mass Spectrometry Study of Electrospray-Generated Ions

Roger Guevremont, K. W. Michael Siu,*,† Jianyao Wang,‡ and Luyi Ding†

Institute for National Measurement Standards, National Research Council of Canada, Montreal Road, Ottawa, Ontario, Canada K1A 0R6

A commercially available ion mobility spectrometer was interfaced to a custom-built linear time-of-flight (TOF) mass spectrometer for the purpose of examining electrospray-generated plumes. Ionic species that were separated in the ion mobility spectrometer could be selectively determined with the TOF mass spectrometer. Tetraalkylammonium salts, a peptide, and proteins were examined. Their ion mobility spectra typically comprised a few peaks; some of these mobility-resolved species produced characteristic electrospray ions, while others of lower relative mobility did not. The TOF mass spectra of cytochrome *c*, injected from the ion mobility spectrometer at an indicated temperature of 90 °C or lower, showed signs that were characteristic of protein−solvent clustering.

Electrospray mass spectrometry is evolving from a scientific curiosity to one of the most powerful tools in the bioanalytical laboratory since Fenn and co-workers' pioneering work on applying this technique to the determination of molecular masses of proteins.[1] As in the development of many analytical techniques, the pace of our understanding of the electrospray process lags far behind the pace at which the technique is being employed in new applications. A difficulty in arriving at a better understanding of the electrospray process, based on the ions that one sees in the electrospray spectrum, is that the spectrum is an accurate picture of only those ions that enter the mass analyser. These are ions that have traveled from a region of 1 atm (the ion source) to another of 1×10^{-5} Torr or lower in pressure, during which their associated solvent molecules, and presumably their molecular adduct components, are stripped by means of a series of collisions with predominately nitrogen and oxygen molecules that enter, along with the analyte ions, into the low-pressure regions of the mass spectrometer. The energy of this collision-induced dissociation (CID) is typically optimized to result in maximal desolvation but minimal decomposition of the analyte ions.[2]

While a spectrum consisting of desolvated ions is desirable for an analysis, it is less so if one wants to learn something about the nature of the ionic species created originally in the electrospray process. In a few studies,[3−5] some knowledge was gained by minimizing the energy of the CID that took place between the orifice and the mass analyser (in the so-called "lens region"). For example, Mirza and Chait[3] reported observation of trifluoroacetic acid adducts of melittin after lowering the potential difference between the transfer capillary and the skimmer of their mass spectrometer. Le Blanc et al.[4] observed ethylamine adducts of gramicidin s after lowering the potential difference between the orifice (OR) and the radio-frequency-only quadrupole (R0) to nominally zero in their mass spectrometer. Adducts between ubiquitin and butylamine were also observed under similar conditions.[5] While these studies provided some information about the ionic species created in the electrospray ion source, this information was still limited because the composition of the ions that entered and exited the lens region was likely to have changed significantly even under mild CID conditions. A support of this speculation is that none of these studies reported observation of solvent (water and/or methanol) adducts, even for experiments in which the potential difference across the lens region was nominally zero.[4]

In an effort to create a second window of observation on the electrospray process, we have elected to insert a separation step, based on differences in ion mobility, between electrospray generation of ions and mass spectrometric detection. Ion mobility spectrometry (IMS), formerly known as plasma chromatography, is a relatively established technique.[6,7] This technique separates gaseous ions on the basis of their different mobilities in a drift gas of relatively high pressure (typically atmospheric). The mobility of an ion is a function of its charge, mass, and physical dimensions.[6,7] For a small ion (ion radius ≪ mean free path), the critical "dimension" is the collision cross section for momentum transfer; for a macroion or a charged droplet (radius ≫ mean free path), drag flow applies, and the relevant dimension is the ion radius, with the gas viscosity coming into consideration. A review of ion mobility is beyond the scope of this paper; interested readers are referred to the two books referenced earlier[6,7] for an introduction of ion mobility and IMS, and the books by McDaniel[8]

† Also with Ottawa−Carleton Chemistry Institute, Carleton University, Ottawa, ON, Canada K1S 5B6.

‡ Current address: Department of Medical Genetics, University of Toronto, Toronto, ON, Canada M5S 1A8.

(1) Mann, M.; Meng, C. K.; Fenn, J. B. *Anal. Chem.* **1989**, *61*, 1702−1708.
(2) Smith, R. D.; Loo, J. A.; Ogorzalek Loo, R. R.; Busman, M.; Udseth, H. R. *Mass Spectrom. Rev.* **1991**, *10*, 359−452.
(3) Mirza, U. A.; Chait, B. T. *Anal. Chem.* **1994**, *66*, 2898−2904.
(4) Le Blanc, J. C. Y.; Wang, J.; Guevremont, R.; Siu, K. W. M. *Org. Mass Spectrom.* **1994**, *29*, 587−593.
(5) Le Blanc, J. C. Y.; Wang, J.; Siu, K. W. M.; Guevremont, R. *Proceedings of the 42nd ASMS Conference on Mass Spectrometry and Allied Topics*; ASMS: Chicago, IL, 1994; p 417.
(6) Carr, T. W., Ed. *Plasma Chromatography*; Plenum Press: New York, 1984; p 259.
(7) Eiceman, G. A.; Karpas, Z. *Ion Mobility Spectrometry*; CRC Press: Boca Raton, FL, 1994; p 228.
(8) McDaniel, E. W. *Collision Phenomena in Ionized Gases*; John Wiley and Sons: New York, 1964; p 775.

S0003-2700(97)00359-4 CCC: $14.00 Published 1997 Am. Chem. Soc.

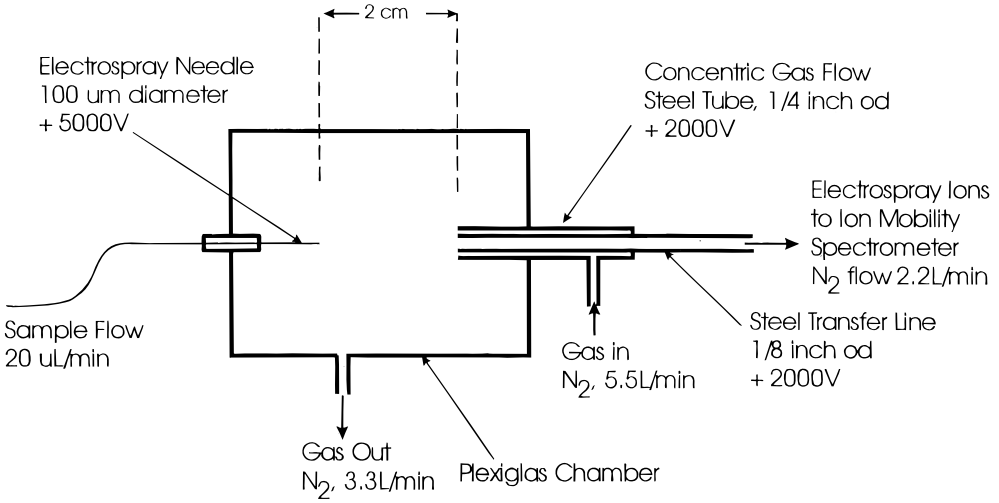

Figure 1. Schematic diagram of the electrospray chamber.

and Mason and McDaniel[9] for an in-depth discussion of the fundamentals of mobility and mobility measurements.

The application of IMS for the detection of electrospray-generated ions dates back to the pioneering work of Dole and co-workers, published in 1984.[10] In the early 1990s, Smith et al.[2,11] reported ion mobility spectra of cytochrome *c* and lysozyme ions in support of their mass spectrometric work. The first full-scale investigation of IMS detection for electrospray was carried out by Hill and co-workers in 1994.[12] These authors reported observation of a number of partially resolved peaks in the ion mobility spectra of cytochrome *c* and Triton X-100. These were interpreted as peaks due to different charge states of cytochrome *c* (+12H to +17H) and Triton X-100 of different monomer units. The first results were of particular importance, as that was "the first time that multiply charged peaks (were) reported in IMS".[12] A subsequent paper from the Hill group[13] described effects of drift tube temperature on the resolution of ion mobility spectra. Partial separation of a mixture of eight alkylamines was reported by Shumate.[14]

The impetus of our current work stemmed from our interest in gaining a better understanding of the ionic species produced in the first instance of electrospray. Therefore, quite apart from gathering mobility data, the primary reason for implementing IMS was to separate these species prior to mass spectrometric detection. Toward that end, we built a linear time-of-flight (TOF) mass spectrometer and coupled it to a commercially available ion mobility spectrometer which had originally been equipped with a quadrupole mass spectrometric detection stage. This change enabled us to collect full-scan mass spectra of individual peaks separated in the ion mobility spectrometer.

Conceptually, our hardware design may be considered to be the reverse of the "ion chromatography" design of Bowers and co-workers[15,16] and the ion mobility apparatus design of Jarrold and co-workers.[17,18] These instruments employ a mass spectral front end to isolate the analyte ions of identical m/z ratios for mobility separation. In contrast, our instrument employs ion mobility separation up front to resolve ionic species for mass spectrometric characterization.

EXPERIMENTAL SECTION

Electrospray. Electrospray was performed at room temperature external to the ion mobility spectrometer. The electrospray needle (~100 μm i.d. stainless steel tube, typically biased to 5 kV) was enclosed in a small Plexiglas chamber (Figure 1). Electrospray-generated ions were swept into the ion source of the ion mobility spectrometer via a stainless steel transfer tube (15 cm in length, $^1/_8$ in. o.d., typically biased to 2 kV) by means of a stream of dry nitrogen. This stream (5.5 L/min) was introduced into the electrospray chamber in a direction countercurrent to that of the electrospray stream. Three-fifths of the nitrogen was vented; the remaining portion was transported into the ion mobility spectrometer. Splitting of the nitrogen flow ensured that only ions and relatively small droplets were admitted into the ion mobility spectrometer. Big droplets were eventually swept out of the electrospray chamber via the vent line.

Ion Mobility Spectrometry/Time-of-Flight Mass Spectrometry. A commercially available ion mobility spectrometry/mass spectrometry (IMS/MS) instrument (PCP Inc., West Palm Beach, FL) was modified to accommodate time-of-flight mass spectrometric detection (Figure 2). The IMS half of the instrument consisted of three ion flight regions, a "reaction region" 5 cm in length, and two "drift regions" each 5 cm in length. The transfer tube from the electrospray source terminated within the reaction region, approximately 2 cm from the first shutter grid. A voltage of 3 kV was applied to the ion mobility spectrometer; since the voltage gradient applied was linear, the resulting bias of the first shutter grid was approximately 2 kV. The voltage applied to the transfer tube was typically optimized for efficient extraction of

(9) Mason, E. A.; McDaniel, E. W. *Transport Properties of Ions in Gases*; John Wiley and Sons: New York, 1988; p 560.
(10) Gieniec, J.; Mack, L. L.; Nakamae, K.; Gupta, C.; Kumar, V.; Dole, M. *Biomed. Mass Spectrom.* **1984**, *11*, 259−268.
(11) Smith, R. D.; Loo, J. A.; Ogorzalek Loo, R. R.; Udseth, H. R. *Mass Spectrom. Rev.* **1992**, *11*, 434−443.
(12) Wittmer, D.; Chen, Y. H.; Luckenbill, B. K.; Hill, H. H., Jr. *Anal. Chem.* **1994**, *66*, 2348−2355.
(13) Chen, Y. H.; Hill, H. H., Jr.; Wittmer, D. P. *Int. J. Mass Spectrom. Ion Processes* **1996**, *154*, 1−13.
(14) Shumate, C. *Trends Anal. Chem.* **1994**, *13*, 104−109.
(15) Kemper, P. R.; Bowers, M. T. *J. Am. Soc. Mass Spectrom.* **1990**, *1*, 197−207.
(16) Bowers, M. T.; Kemper, P. R.; von Helden, G.; van Koppen, P. A. M. *Science* **1993**, *260*, 1446−1451.
(17) Jarrold, M. F. *J. Phys. Chem.* **1995**, *99*, 11−21.
(18) Clemmer, D. E.; Hudgins, R. R.; Jarrold, M. F. *J. Am. Chem. Soc.* **1995**, *117*, 10141−10142.

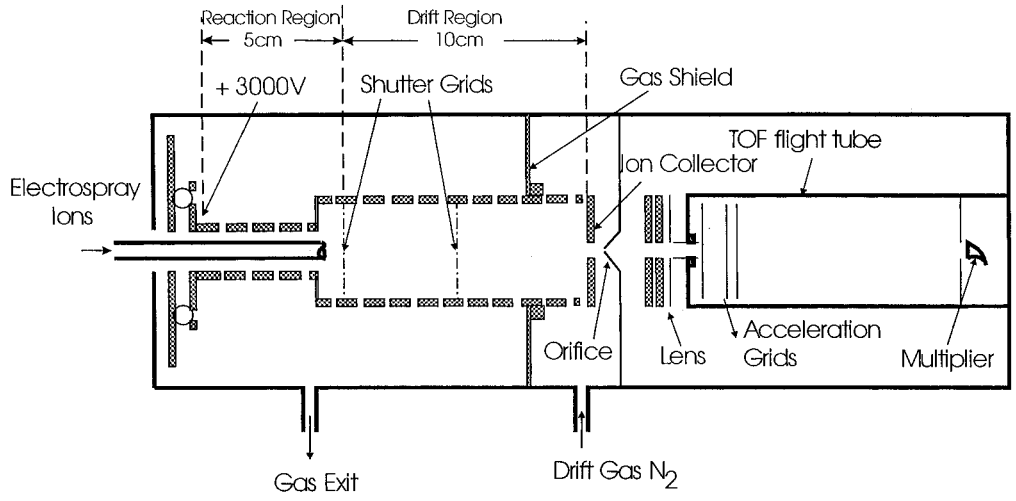

Figure 2. Schematic diagram of the ion mobility spectrometer/time-of-flight mass spectrometer.

electrospray-generated ions from the transfer tube to the shutter grid using the ion mobility signal as the guide. The optimum voltage was approximately 2 kV, with a usable range of ±50 V.

As previously mentioned, the ion mobility spectrometer shown in Figure 2 had two drift regions in series and shutter grids at the entrances to these drift regions. Since the transfer tube from the electrospray chamber ended 2 cm from the first shutter grid, the gas turbulence due to the nitrogen flow in the region decreased the effectiveness of this shutter grid. Consequently, the first shutter grid was left in the open state for all of the work described here. Ions exiting from the transfer tube crossed the first shutter grid and traversed the first drift region without separation. The second shutter grid was closed most of the time but opened briefly to permit a sample of ions to pass into the second drift region. A countercurrent stream of nitrogen (the "drift gas", 0.5 L/min) flowed from the detector end of the ion mobility spectrometer toward the entrance. This flow reduced the solvent load in the drift regions and ensured that ions traversed in a gas that was thermally equilibrated with the spectrometer.

The ion mobility spectrometer was operated in the conventional manner albeit with one exception: the period during which the second shutter grid was open (the width of the gating function) was extended from the typical 0.1 ms up to 5 ms to accommodate the low-mobility ions of interest in this study. This resulted in good sensitivity for detection of ions with mobility as low as 0.2 $cm^2\ V^{-1}\ s^{-1}$ (e.g., cluster ions); however, ions with high mobility were recorded as square-top peaks (see, for instance, Figure 3). This feature was not a consequence of detector saturation but one of a steady flux of ions passing through the shutter grid during the relatively long time that the grid was open; the sharp rising and falling edge signified the rapid opening and closing of the grid. The ion transit time across the drift region (from which the ion mobility was calculated) was measured from the time that the grid was open to the time of the half-maximum of the rising edge. For Gaussian peaks, the ion transit time was measured in the conventional manner, i.e., from the time at the middle of the period during which the shutter grid was open to the time of the peak maximum. The ion current arriving at the ion collector (about a few tens of picoamperes) was amplified by means of a wide-band electrometer and recorded with a synchronous signal averager. The ion mobility spectrometer was typically operated at a temperature of 150−200 °C. A linear TOF mass spectrometer, with its associated lens and grids, was installed and replaced the quadrupole mass spectrometer of the original instrument (Figure 2). Ions exiting the ion mobility spectrometer (at 1 atm) entered the vacuum system through an orifice of approximately 25 μm in diameter. These ions were steered into the flight area by means of four lens elements and accelerated using two simultaneous pulses (pulse generator, Directed Energy Inc., Fort Collins, CO, Model GRX-3.0K-H) applied to two grids approximately 5 cm apart. The lens elements were typically biased to −370, −370, −385, and −400 V, starting from the orifice side. Typical pulse amplitudes were +1800 V to the first and +1710 V to the second grid; the pulse widths were 5 μs. The ions then passed through a third grid held at ground potential located 1 cm downstream. The amplitudes of the pulses applied to the two acceleration grids were optimized to give a focused signal at the mass spectrometric detector. Ions that were originally at the first acceleration grid would receive the largest acceleration, while those that were originally at the second grid would receive the smallest; the amplitudes of the pulses were adjusted such that these ions would arrive at the detector simultaneously. The individual IMS peaks could be "gated" for TOFMS. This was achieved by acquiring data only when the IMS peak of interest reached the TOF mass spectrometer.

The TOF instrument was evacuated by means of two diffusion pumps: the first one, 2400 L/s (Varian, Model VHS-6, Lexington, MA), was located beneath the orifice, and the second one, 2500 L/s (Edwards High Vacuum International, Model 250, West Sussex, England), was located beneath the TOF flight tube. The typical operating pressure in the TOF flight tube was 1×10^{-5} Torr.

An electron multiplier (ETP Electron Multipliers, AF850, Ermington, Australia) was used to detect the ions. Typically, the multiplier was biased to −1.8 kV, while the conversion dynode voltage was maintained at −2.5 kV. The pulse width of individual ions detected was <0.1 μs. The optimum width of a TOF peak was about 0.3 μs for this instrument. A Lecroy digital storage oscilloscope (Model 9350, Chestnut Ridge, NY) was used to collect and process the TOF mass spectra.

Samples were solutions of tetraalkylammonium bromide (2.5 mM), gramicidin s (0.5 mM), bovine ubiquitin (50 μM), bovine insulin (100 μM), and equine cytochrome *c* (50 μM) (all chemicals

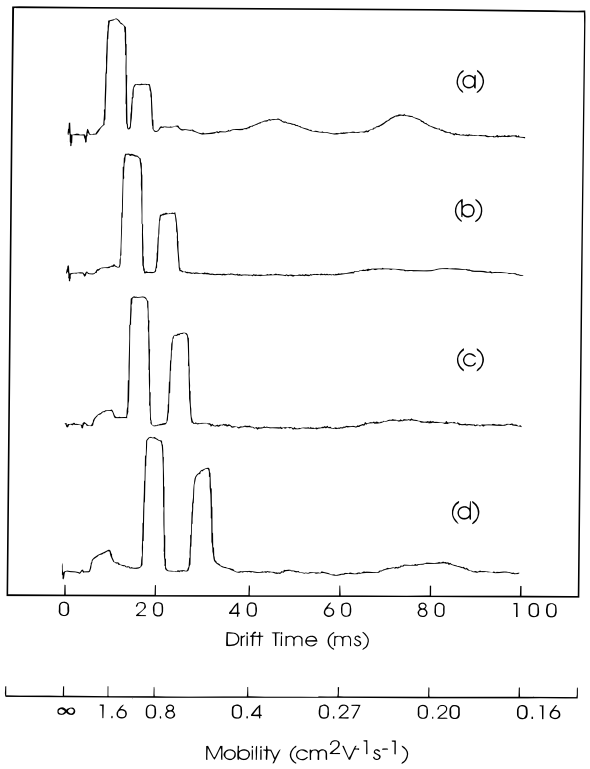

Figure 3. Ion mobility spectra of tetraalkylammonium bromides: alkyl = (a) ethyl, (b) butyl, (c) pentyl, and (d) heptyl. IMS temperature, 150 °C. In this and subsequent figures, the mobility scale shows reduced mobility, K_0.

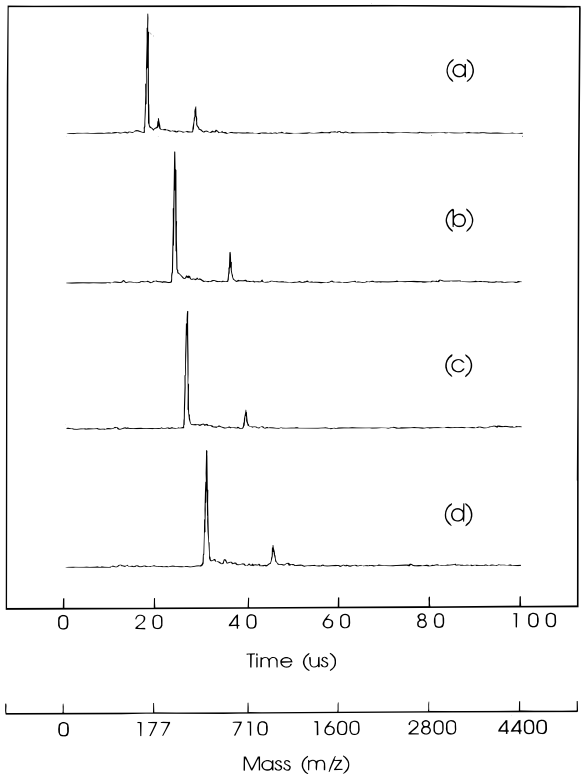

Figure 4. Time-of-flight mass spectra of tetraalkylammonium bromides whose ion mobility spectra are shown in Figure 3: alkyl = (a) ethyl, (b) butyl, (c) pentyl, and (d) heptyl.

available from Sigma Chemical Co.), prepared in 50/50 methanol/water; protein and peptide solutions were adjusted to pH 3 with acetic acid.

RESULTS AND DISCUSSION

Tetraalkylammonium Salts. We began with an examination of tetraalkylammonium salts because they had been examined previously by means of both mass spectrometry[19] and ion mobility spectrometry.[12] Figure 3 shows the ion mobility spectra, while Figure 4 shows the corresponding TOF-MS spectra of four tetraalkylammonium (here, alkyl = ethyl, butyl, pentyl, and heptyl) bromide samples. Note that these results were obtained without "gating" of the IMS peaks and that the TOF spectrum was a composite of all the ions that reached the mass spectrometer. The identity of the individual IMS peak was determined by collecting spectra only during the period when ions of that peak arrived at the orifice of the TOF mass spectrometer. An example is shown in Figure 5 for tetraoctylammonium bromide. In general, only two abundant ions were seen for tetraalkylammonium samples, M^+ and $M(MBr)^+$. Higher adducts, $M(MBr)_n^+$, where $n = 2$ or higher, were observed in some cases, e.g., tetraoctylammonium bromide shown in Figure 5.

Figure 5b shows the composite TOF mass spectrum of the IMS ions; the following ions are discernible: M^+, $M(MBr)^+$, and $M(MBr)_2^+$. The TOF mass spectra obtained from gating the IMS peaks, A−D, are shown in Figure 5c−f. Evidently, peak A is M^+, peak B is $M(MBr)^+$, and peak C is $M(MBr)_2^+$; the $M(MBr)^+$ ion seen in Figure 5e could originate from the tail of peak B, but it is more likely from fragmentation of $M(MBr)_2^+$. Every attempt to collect mass spectra of relatively low mobility ions, such as peak D, failed to produce characteristic ions; this means that our mass spectrometric measurements were of insufficient sensitivity and/or range for the ions of those m/z ratios (upper limit measured = 4000). In spite of this, some properties of these ions are discernible from the mobility spectrum in Figure 5a. Peak D has a maximum at 75 ms and a range of 63−90 ms; these correspond to a most probable reduced mobility, K_0 (see later sections for definition), of 0.22 $cm^2\ V^{-1}\ s^{-1}$ and a range of 0.18−0.26 $cm^2\ V^{-1}\ s^{-1}$. That this peak is relatively broad (in comparison with peaks A−C) suggests that it is likely to be comprised of a mixture of ions and possibly of varying dimensions and charges (two key parameters upon which ion mobility is dependent). Knowledge of one defines the other. For peak D, if the net charge of these ions is +1, the corresponding ionic radius range is 1.3−1.5 nm (see Millikan's equation in the Appendix); however, if the net charge is +50, the range becomes 64−77 nm. Although the exact nature of these ions is not known, it is tempting to assign these ions as "clusters" or "charge residues" from evaporating electrospray-generated droplets, which are believed to have a relatively narrow size distribution.[20]

Gramicidin s. Figure 6 displays the results for gramicidin s. The IMS spectrum shown in Figure 6a comprises three peaks, A−C. The composite TOF mass spectrum in Figure 6b shows the characteristic $[M + H]^+$ and $[M + 2H]^{2+}$ ions of gramicidin. Gating of peak A identified it as $[M + 2H]^{2+}$ and peak B as $[M + H]^+$. Gating of peak C produced no characteristic ions.

Ubiquitin. The spectra of ubiquitin were comparatively simple. The ion mobility spectrum showed three peaks: a small first peak (K_0 = 1 $cm^2\ V^{-1}\ s^{-1}$) comprising solvent clusters; a

(19) Yamashita, M.; Fenn, J. B. *J. Phys. Chem.* **1984**, *88*, 4451−4459.

(20) Kebarle, P.; Tang, L. *Anal. Chem.* **1993**, *65*, 972A−986A.

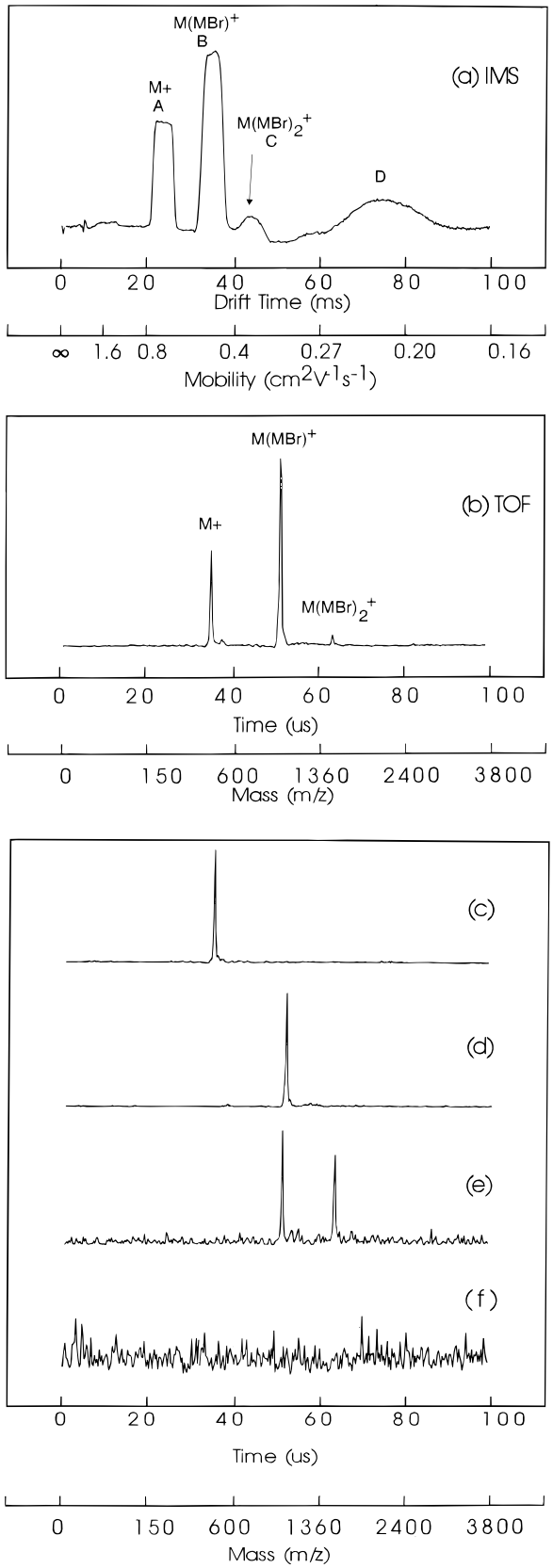

Figure 5. Tetraoctylammonium bromide: (a) ion mobility spectrum at 150 °C; (b) composite TOF mass spectrum; (c) TOF mass spectrum of peak A; (d) TOF mass spectrum of peak B; (e) TOF mass spectrum of peak C; (f) TOF mass spectrum of peak D.

relatively large and broad second peak (K_0 = 0.7 cm^2 V^{-1} s^{-1}), gating of which revealed a multiply charged ubiquitin ion distribution from $[M + 5H]^{5+}$ to $[M + 11H]^{11+}$; and a very broad but

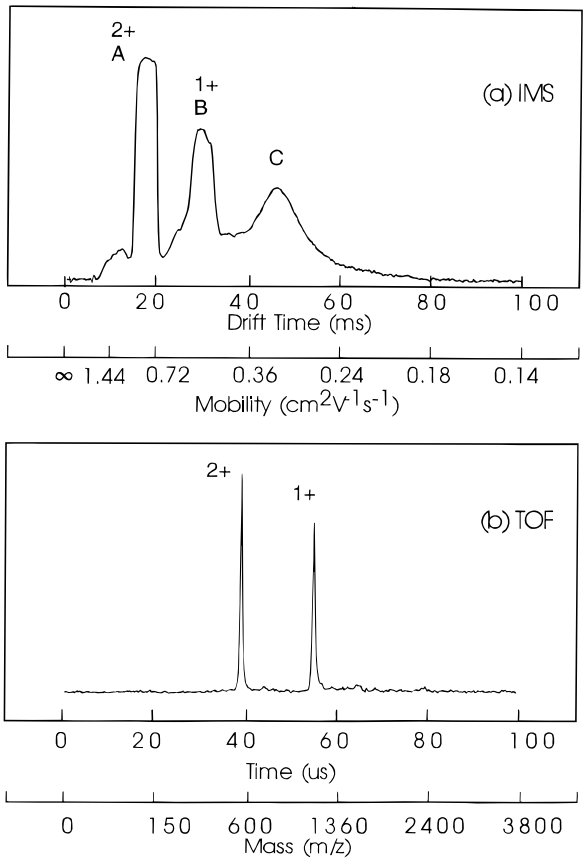

Figure 6. Gramicidin s: (a) ion mobility spectrum at 200 °C; (b) composite TOF mass spectrum.

short third peak (K_0 = 0.25 cm^2 V^{-1} s^{-1}), gating of which produced no characteristic ions.

Insulin. Figure 7 shows the results for insulin. Three relatively broad peaks (A −C) were observed in the IMS spectrum (Figure 7a) of this protein. The composite TOF mass spectrum shows the $[M + 3H]^{3+}$, $[M + 4H]^{4+}$, and $[M + 5H]^{5+}$ ions of insulin (Figure 7b). Gating of peak A produced a similar TOF spectrum. Gating of peak B yielded no characteristic ions other than the multiply charged insulin ions, which may have originated from the tail of peak A. No characteristic ions were identifiable in the mass spectrum of peak C.

Cytochrome *c*. All of the above data were gathered with an indicated ion mobility spectrometer temperature of 150−200 °C. For cytochrome *c*, measurements were carried out under a wide series of IMS temperatures: 30, 60, 90, 120, 150, 180, and 200 °C. The IMS spectra obtained under three selected temperatures are shown in Figure 8a. Gating the three IMS peaks revealed that peak A contained solvent ions and peak B cytochrome *c* ions; peak C produced no observable ions. The corresponding TOF mass spectra are displayed in Figure 8b. An effect of increasing temperature was decreases in mass spectral peak width and *m/z* values; this change was also accompanied by a concomitant increase in ion abundances. We interpret the decrease in mass spectrometric peak width and *m/z* values with increasing temperature from 30 to 90 °C and higher as an indication of thermal declustering of cytochrome *c* ions in the ion mobility spectrometer. That is to say, the cytochrome *c* ions reaching the TOF mass spectrometer were in a lower degree of solvation for a higher IMS temperature than those for a lower temperature, since mass spectrometric conditions were constant. This interpretation is

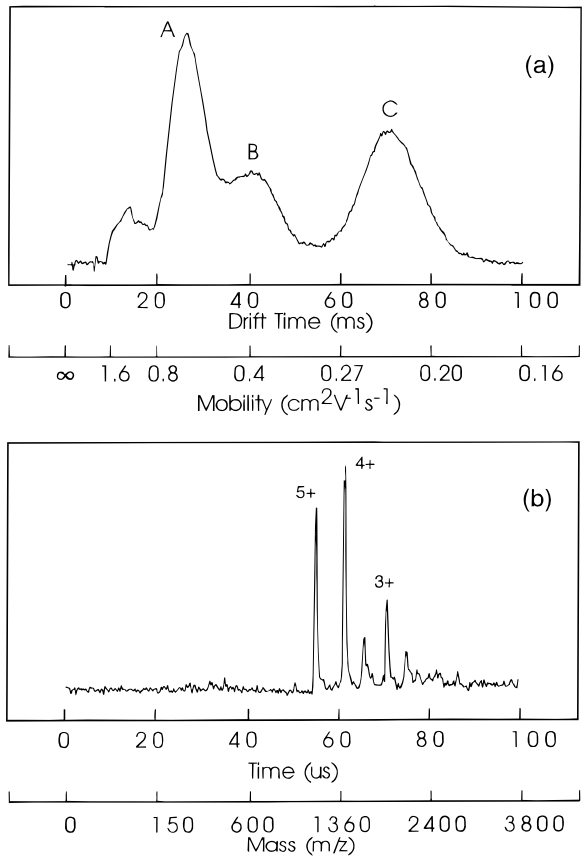

Figure 7. Insulin: (a) ion mobility spectrum at 150 °C; (b) composite TOF mass spectrum.

consistent with that of Hill and co-workers,[13] who observed a dramatic improvement in the resolution of their ion mobility spectra with increasing temperature and attributed that effect to increasing ion desolvation. Furthermore, our IMS/TOF interface conditions must have been relatively inefficient in declustering protein ions, since electrospraying the same cytochrome *c* sample at room temperature in a commercial mass spectrometer, e.g., the Sciex TAGA 6000E, produces a mass spectrum of declustered, multiply charged cytochrome *c* ions.

The IMS spectra in Figure 8a showed that ions' drift times changed, and therefore their mobilities (*K*s) changed, with changing temperature. Mobility is related to the drift time as follows:[6,7]

$$K = L^2/(t_d V)$$

where L is the length of the drift tube, t_d the drift time, and V the applied potential. Most of the changes were a consequence of the decrease in gas density with increasing temperature. To compare *K*s measured under different temperatures, they may be converted to reduced mobilities, K_0s:[8,9]

$$K_0 = K(273/T)(P/760)$$

where T is the absolute temperature and P is the pressure. The K_0s of peaks A−C (three are shown in Figure 8a) are plotted against temperature in Figure 9. As discussed earlier, we interpret the mass spectral changes on increasing temperature shown in Figure 8b as an indication of thermal declustering. If this

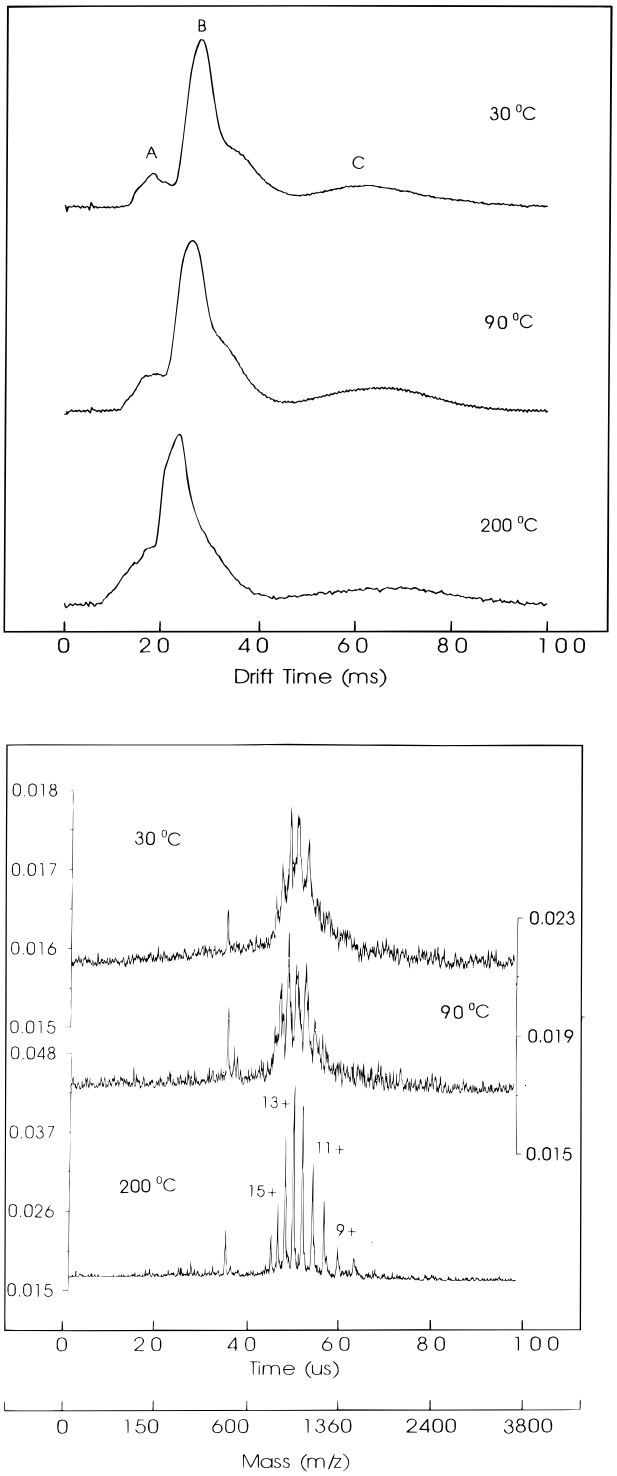

Figure 8. (a) Ion mobility spectra of cytochrome *c* at 30, 90, and 200 °C. (b) Corresponding time-of-flight mass spectra at 30, 90, and 200 °C.

occurred, there would be a reduction in ion size and a concomitant increase in mobility, provided the change was not masked by any intrinsic thermal dependence of K_0. This dependence reflects the nature of the ion−neutral interaction and need not be a monotonic function;[9] furthermore, even for members of a homologous series of compounds (e.g., amines), measured reduced mobilities exhibit a temperature dependence that is mass-related.[7,22] For amines,

(21) Annis, B. K.; Malinauskas, A. P.; Mason, E. A. *Aerosol Sci.* **1972**, *3*, 55−64.
(22) Karpas, Z. *Anal. Chem.* **1989**, *61*, 684−689.

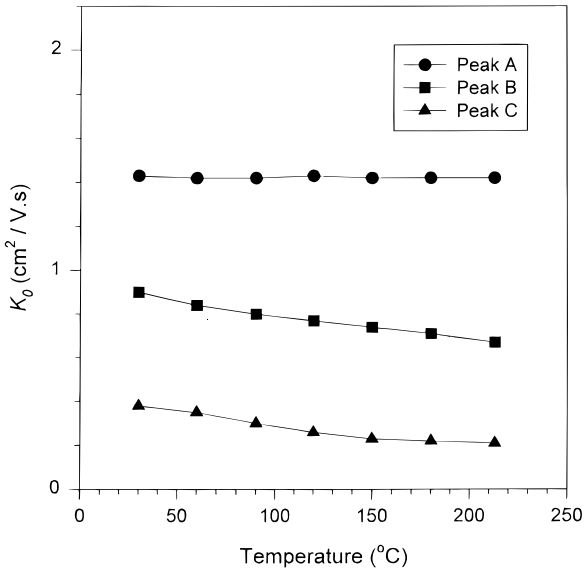

Figure 9. Temperature dependence of reduced mobilities of cytochrome *c* peaks: peaks A, B, and C identified in Figure 8a.

the temperature dependence is positive (i.e., reduced mobility increases with increasing temperature) for low molecular mass ions, is essentially invariant for intermediate mass (90−180 Da) ions, and is negative for heavy ions.[22] The data in Figure 9 show that, for peak A, its reduced mobility was insensitive to temperature changes, while for peaks B and C, their reduced mobilities decreased with increasing temperature. (Similar trends were also observed for ubiquitin [data not shown].) From what we know about the nature of the species within peaks A−C, these trends appear to agree with those of the amine study.[22] Efforts in distilling declustering information from the IMS spectra and correlating mobility and mass spectral information are now underway.

Comparison with Other IMS Studies. Table 1 is a comparison of the K_0s of the M^+ ions of the tetraalkylammonium ions, most of which are shown in Figure 3, with the corresponding K_0s reported in ref 12. It is apparent that the two sets of reduced mobilities are quite similar. A plot of the inverse reduced mobilities versus the ionic masses of this homologous series of ions yielded a linear plot (not shown); similar plots of other homologous series have previously been reported.[7]

Qualitatively, the protein IMS spectra obtained in this study resemble more closely those reported by Smith et al.[2,11] than those by Hill and co-workers.[12,13] The IMS peaks are relatively broad[2,11] and lack the "fine" features reported by the Hill group.[12,13]

Table 1. Reduced Mobilities (K_0, cm^2 V^{-1} s^{-1}) Previously Reported[12] and Measured in This Study[a]

		K_0	
cation	mass (Da)	ref 12	this work
tetraethylammonium	130.3		1.88
tetrabutylammonium	242.5	1.19	1.31
tetrapentylammonium	298.6	1.03	1.12
tetrahexylammonium	354.7		0.99
tetraheptylammonium	410.8	0.81	0.89
tetraoctylammonium	466.9		0.80

[a] P = 760 mmHg; T = 423 K.

Furthermore, both Smith et al.[2,11] and we observed multiple protein-related IMS peaks; we proved that the higher mobility species is (solvated) protein, and we demonstrated by means of their mass spectra that the degree of solvation decreases with increasing IMS temperature. On the surface, our inability to observe protein ions in gating experiments of the lower mobility species appears to confirm the Smith group's assertion that these species "do not contribute to conventional (electrospray) mass spectra"; however, as we previously discussed, our IMS/TOF interface appears to be relatively inefficient in desolvating the protein ions and, therefore, by extension, would be relatively inefficient in performing declustering of protein "particles" or multimers, if these were, indeed, present. We shall reserve judgement on this issue until future data warrant it.

ACKNOWLEDGMENT

Parts of this study were reported in the annual conferences of the American Society for Mass Spectrometry; 42nd, Chicago, IL, May 29−June 3, 1994; 43rd, Atlanta, GA, May 21−26, 1995; and 44th, Portland, OR, May 12−16, 1996.

APPENDIX

The mobility, K, is related to the charge, q, and radius of the ion, R, by Millikan's equation:[21]

$$K = \frac{q}{6\pi\eta R}\left[1 + \frac{\lambda}{R}(A + B\mathrm{e}^{-cR/\lambda})\right]$$

where η is the gas viscosity and λ is the mean free path; A, B, and C are constants and equal 1.234, 0.414, and 0.876, respectively.

Received for review April 3, 1997. Accepted July 3, 1997.[⊗]

AC970359E

[⊗] Abstract published in *Advance ACS Abstracts,* August 15, 1997.